Journal of Colloid and Interface Science **249,** 30–43 (2002)
doi:10.1006/jcis.2001.8114, available online at http://www.idealibrary.com on IDEAL®

Hybrid Monte Carlo Method for Simulation of Two-Component Aerosol Coagulation and Phase Segregation

Y. Efendiev*,[1] and M. R. Zachariah†,[2]

*Institute for Mathematics and Its Applications; and †Departments of Mechanical Engineering and Chemistry, University of Minnesota, Minneapolis, Minnesota 55455

Received May 29, 2001; accepted November 24, 2001; published online March 26, 2002

The paper presents the development of a hybrid Monte Carlo (MC) method for the simulation of the simultaneous coagulation and phase segregation of an immiscible two-component binary aerosol. The model is intended to qualitatively model our prior studies of the synthesis of mixed metal oxides for which phase-segregated domains have been observed in molten nanodroplets. In our previous works (*J. Aerosol Sci.* 32, 1479 (2001); *Chem. Eng. Sci.* 56, 5763 (2001); submitted for publication) we developed sectional and monodisperse models where the internal state of the aerosol particles was described. These methods have certain limitations and it is difficult to include additional physical effects into the framework. Our new approach combines both constant volume and constant number Monte Carlo methods. Similar to our previous models, we assume that the phase segregation is kinetically controlled. The MC approach allows us to compute the mean number of enclosures (minor phase) per droplet, average enclosure volume, and the width of the enclosure size distribution. The results show that asymptotic behavior of enclosure distribution exists that is independent of initial conditions, which is very close to the continuum self-preserving distribution. Temperature is a key parameter because it allows for a significant change in the internal transport rate within each droplet. In particular, increasing the temperature significantly enhances the Brownian coagulation rate and lowers the number of enclosures per droplet. As a result, the MC results indicate that the growth of the minor phase can be moderated quite dramatically by small changes in system temperature. These results serve to illustrate the utility of this synthesis approach to the controlled growth of nanoparticles through the use of a majority matrix to slow down the encounter frequency of the minor phase and therefore its particle size. © 2002 Elsevier Science (USA)

Key Words: **nanoparticles; simulation.**

1. INTRODUCTION

Aerosol growth processes and in particular aerosol dynamics modeling have generally been limited to single-component (on a molecular or phase basis) systems. Furthermore, even those studies that have employed more than one component assume that the aerosol is a homogeneous mixture of all the multicomponent constituents. However, we know that phase segregation will take place within an aerosol droplet if the thermodynamics and kinetics are favorable in a manner analogous to that observed in bulk materials. We have been involved in a number of multicomponent aerosol dynamics studies with heterogeneous aerosol particles. One of our main goals in this research is to study the evolution of the internal state of the aerosol droplets. For example, we have conducted studies on the formation of binary metal oxide systems with application to removal of heavy metals (1, 2) as well as the formation of materials with novel and interesting properties (3–5).

Our initial success in growing interesting microstructures (6) indicated that further research into the mechanistic aspects of the growth was warranted. In subsequent studies we employed *in situ* interrogation into the formation process (7), multicomponent aerosol dynamic modeling (8), and molecular dynamics computation (9). One of the primary conclusions was that, at the high temperatures where these materials are typically grown, nanodroplets are in a liquid-like state and that phase segregation taking place within the nanodroplet was probably limited by transport within the nanodroplet.

In the course of this paper we shall use the terms minor phase and enclosure interchangeable to refer to the component within each aerosol droplet and droplet or aerosol when referring to the major phase. The mathematical formulation of the problem allows one to consider the enclosures as particles inside the droplet, where the minor-phase growth takes place due to continuum interception and the major-phase growth (the aerosol phase) takes place due to free molecule coagulation. The temporal evolution of the aerosol and enclosures is schematically depicted in Fig. 1. Because our experimental studies were all undertaken when both components were in the molten state, we only observed spherical droplets for both the major and the minor phase, which also justifies the use of an instantaneous coalescence assumption in our model.

In our previous work (10) we developed a 2D sectional model to describe the aerosol droplets and their internal state and employed basic statistics to describe the enclosure population inside the droplet. That model was limited in that it was strictly valid only if the mean volume of the enclosures in a droplet were

[1] Current address: Texas A&M University, Department of Mathematics, College Station, Texas 77843.

[2] To whom correspondence should be addressed.

0021-9797/02 $35.00
© 2002 Elsevier Science (USA)
All rights reserved.

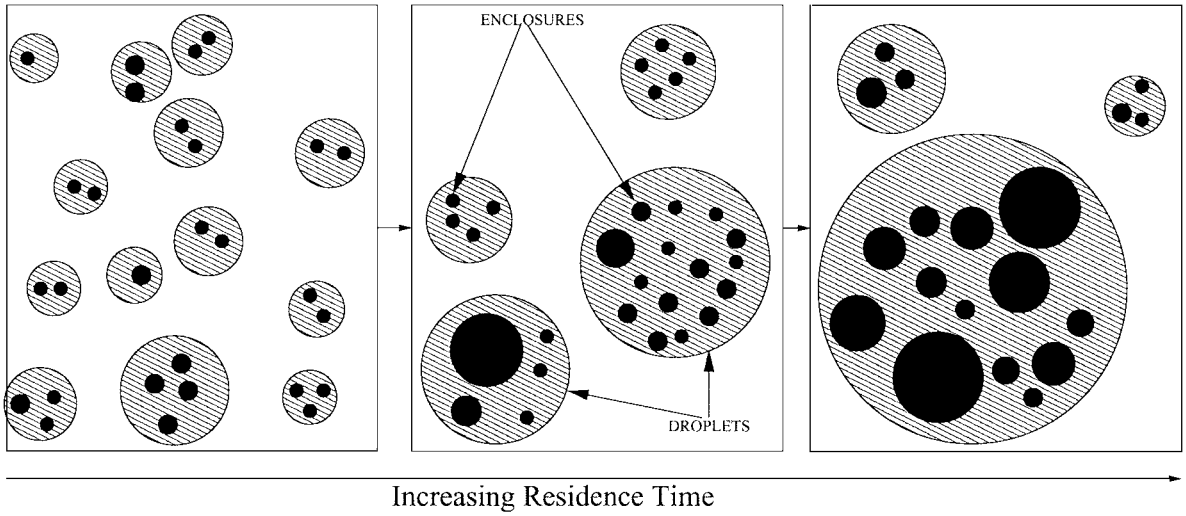

FIG. 1. Schematic description of the droplet–enclosure growth process.

the same for each droplet at any instant in time. The use of a sectional approach also makes it more difficult to introduce additional effects without significant reformulation of the general structure of the aerosol general dynamic equation (GDE).

Monte Carlo methods have the advantage that multiscale and time phenomena can be simultaneously solved without the requirement of a single unifying governing multivariate equation. Moreover, Monte Carlo methods provide an intuitive tool for simulating discrete systems and allow us to study finite size effects and spatial correlations. In the simulation of heterogeneous aerosols Monte Carlo methods are also attractive because they do not require any a priori assumptions about the enclosure distribution in each droplet. In this paper we propose a hybrid Monte Carlo technique to describe the growth of the heterogeneous aerosol particles and their internal state. This approach combines two MC simulations; one simulates the coagulation of the droplets and the other simulates the interaction between the enclosures.

The Monte Carlo model developed in the paper is applied to our experimental observations of the binary SiO_2/Fe_2O_3 system, where SiO_2 is the major phase and Fe_2O_3 is the minor phase (3, 5). An example of TEM results for the SiO_2/Fe_2O_3 system is in Fig. 2. We can see that at short residence times the dark Fe_2O_3 enclosures are greater in number and smaller in size than those observed at longer residence times. It should be reiterated that when growing, both phases are in a liquid state (high-temperature growth) and aerosol droplets consist of two immiscible components (based on known phase behavior). These latter points provide the justification for a model based on transport-limited growth. Our goal is to determine the distribution of the droplet volumes and the internal state of the droplet as a function of time. Using our Monte Carlo approach, we calculate various statistical quantities, such as mean number of the enclosures per droplet, mean enclosure volumes of each droplet, average enclosure volume, normalized second moment of the enclosures, etc., and show that their asymptotic behavior are independent of time. Some of these quantities describe the effect of the major phase on the growth of the enclosures and others allow us to find the nature of the enclosure size distribution. In particular, our computations reveal that the enclosure distribution reaches the self-preserving size distribution. Another interesting observation is that the normalized variance of the mean enclosure volumes in each droplet reaches an asymptotic value, which depends on the temperature. Interestingly, the distribution of the mean enclosure volumes of each droplet can behave very differently from the distribution of the droplet volumes at low temperatures.

In the next section we briefly describe the mathematical (continuous) model and the general framework that we have employed in our previous works to model the aerosol growth and their internal structure. In Section 3 we describe the hybrid MC algorithm and in Section 4 we discuss the implementation of the algorithm. Finally, the numerical results and observations are presented in Section 5.

2. MATHEMATICAL MODEL

The particle size distribution of a polydisperse aerosol undergoing coagulation is governed by the integro-differential equation

$$\frac{dN(t,V)}{dt} = \frac{1}{2}\int_0^V K(U, V-U)N(t,U)N(t,V-U)\,dU - N(t,V)\int_0^\infty K(V,U)N(t,U)\,dU, \qquad [1]$$

where $N(t, V)$ is the particle size distribution function at time t and $K(U, V)$ is the collision frequency function for two particles with volume U and V. The appropriate form of the collision frequency function depends on the type of collision environment in

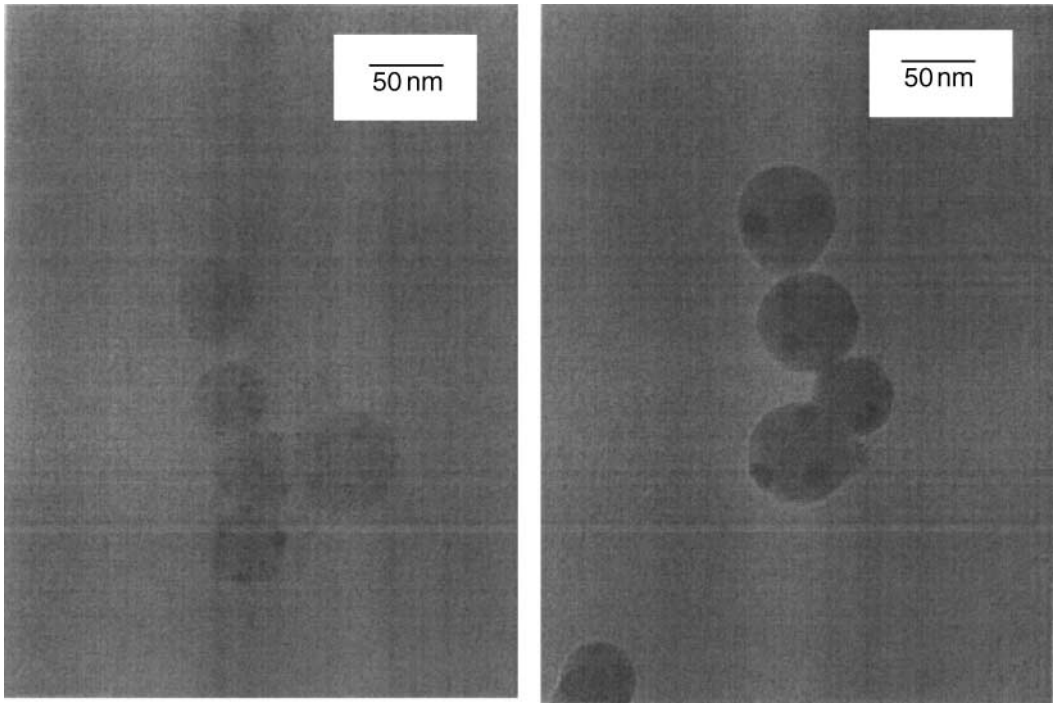

FIG. 2. Evolution of the aerosol (SiO_2) and minor phase (Fe_2O_3) during the growth of SiO_2/Fe_2O_3 nanocomposites.

which the particles exist. In particular, the free-molecule regime coagulation is given by

$$K^F(U,V)=\left(\frac{3}{4\pi}\right)^{1/6}\left(\frac{6kT}{\rho}\right)^{1/2}\left(\frac{1}{U}+\frac{1}{V}\right)^{1/2}\left(U^{1/3}+V^{1/3}\right)^2, \quad [2]$$

for the continuum regime is given by

$$K^D(u,v)=\frac{2kT}{3\mu}\left(u^{1/3}+v^{1/3}\right)\left(\frac{1}{u^{1/3}}+\frac{1}{v^{1/3}}\right), \quad [3]$$

Here, k denotes Boltzmann's constant, T is the temperature, μ is the viscosity of the medium comprising the droplets, and ρ is the density of droplets. Of particular note is that the collision frequency function in the free-molecule regime is relatively independent of temperature. As a result, the growth rate of an aerosol cannot be significantly impacted through changes in temperature. By contrast, Brownian coagulation depends on viscosity, which can for some working fluids be quite temperature sensitive. So that while a gas is not very sensitive to temperature, a liquid can be, and we might consider that one could control the growth of particles if they are embedded within a viscous fluid comprising an aerosol droplet.

Following our previous works, we assume that the droplets coagulate in a free-molecular regime, while the enclosures grow/coagulate in a continuum regime. Denoting the number density of the enclosures in a droplet with volume V, by $n_V(u,t)/V$, we can write a population balance equation for the enclosures,

$$\frac{dn_V(t,v)}{dt}=\frac{1}{2V}\int_0^v K^D(u,v-u)n_V(t,u)n_V(t,v-u)\,du - \frac{1}{V}n_V(t,v)\int_0^\infty K^D(v,u)n_V(t,u)\,du. \quad [4]$$

Note that $n_V(u,t)\,du$ is the number of enclosures with volume between u and $u+du$ in the droplet of volume V. In general, to find the enclosure distribution for the whole system, one needs to add the enclosure distributions over all droplets:

$$n^{total}(u,t)=\int_0^\infty n_V(u,t)N(V,t)\,dV. \quad [5]$$

Here, we denote by $n^{total}(u,t)$ the enclosure distribution of the whole system and $N(V,t)$ the number density of the droplets. Since Eq. [4] is nonlinear and the operation [5] is linear, one cannot derive an equation for the evolution of $n^{total}(u,t)$ analytically. Moreover, since the number of the droplets in the system is typically very large, it is impossible to simulate the individual enclosure interaction in each droplet separately.

In our previous work (10, 11), we developed a 2D general dynamic equation that accounts for the enclosure distribution in each droplet. In particular, we look for the evolution of $N_m(V,t)$, where $N_m(V,t)\,dV$ is the number of droplets with volume between V and $V+dV$ and with m enclosures. The evolution of

$N_m(V,t)$ is given by

$$\frac{dN_m(t,V)}{dt} = \frac{1}{2}\int_0^V \sigma(U, V-U)\sum_{k=1}^{m-1} N_k(t,U)N_{m-k}(t,V-U)\,dU - N_m(t,V)\int_0^\infty \sigma(U,V)\sum_{k=1}^{\infty} N_k(t,U)\,dU + \sum_{k=m+1}^{\infty}\gamma_{k\to m}N_k(t,V) - \sum_{k=1}^{m-1}\gamma_{m_i\to k}N_m(t,V). \quad [6]$$

The quantity $\gamma_{k\to m}\,dt$ denotes the probability that in a droplet of volume V the number of enclosures will change from n to m during the time dt. The first two terms in Eq. [6] account for the gain and loss due to agglomeration of droplets, while the last two terms refer to the gain and loss due to interaction of the enclosures inside a droplet of volume V.

Modeling of $\gamma_{k\to m}\,dt$ usually requires additional assumptions since in general one cannot model the details of the enclosure size distribution without complete knowledge of particle size distribution. The 2D GDE system presented above was solved by a sectional representation of Eq. [6] with an assumption of either monodisperse (11) or log-normally distributed enclosures (10).

One of the advantages of MC approaches is that we do not require any a priori assumption about the enclosure distribution in each droplet.

3. HYBRID MONTE CARLO (MC) MODEL

Monte Carlo methods to simulate particulate growth processes are not new, and the theoretical foundations have been discussed extensively in the literature (12–17). Basically, the Monte Carlo approach utilizes probabilistic tools to study a finite dimensional subsystem to infer the properties of the whole system. It has been shown rigorously (18) that the Monte Carlo approach approximates the integro-differential GDE for the number concentration of particles of any given size as a function of time.

There are a number of Monte Carlo techniques that have been developed for the growth of dispersed systems and generally fall into the class of constant-number or constant-volume methods. There are in general two types of finite-volume Monte Carlo techniques. In the first approach the user sets the time interval Δt and uses Monte Carlo to decide which and how many events will be realized. This method is sometimes referred to as time-driven Monte Carlo. In the second approach, the user selects a single event and then advances the time by an appropriate increment. In the method presented here we employ the first method for the enclosures or minor phase and the second method to describe the droplets/aerosol. More precisely, we first select a single coagulation event for the droplets and compute the time ΔT required for this event. Then, for each droplet we calculate the enclosure interactions that occurred during this time interval.

The finite number of particles used in the simulation introduces certain limitations. Assuming the simulation begins with N particles initially, then after $N-1$ coagulation events, there is one particle left, and the simulation must be terminated. In general, the accuracy of Monte Carlo is proportional to $1/\sqrt{N}$, where N is the number of particles in the system. Thus, in practice, the simulation must be terminated well before the formation of one particle to preserve the accuracy of the calculation. To circumvent the problem, previous workers (19, 20) have developed MC algorithms where the number of particles are kept constant by adding a new particle at each time step or by topping up the system (doubling the number of particles) when the number of particles has dropped to half the initial value. We refer to this MC approach as constant-number MC method.

In simulating heterogeneous aerosols, we need to describe both the internal state of the aerosol droplets and their growth. For the droplets we employ a finite-number Monte Carlo and top up our system when the number of particles are halved. For the internal state of the droplets we employ the finite-volume Monte Carlo approach and following each droplet coagulation calculate the successful enclosure interactions in each droplet. Note that to model the internal state of the droplets, we need complete knowledge of the enclosure distribution in each droplet. In our previous work the internal state of the droplets employed an a priori assumption about the size distribution. Here, however, we wish to relax this constraint to track the evolution of the higher statistical moments. The MC approach allows us to compute higher moments of the distribution without the need to make a priori assumptions about the size distribution.

At each step of the simulation, droplets i with volume V_i and j with volume V_j are selected to coagulate, and a new droplet of size $V_i + V_j$ is formed with a probability that is proportional to the coagulation probability, K_{ij}. In the free-molecule regime, the collision probability is proportional to $K_{ij}^F = K^F(V_i, V_j)$ and in the continuum regime to $K_{ij}^D = K^D(V_i, V_j)$.

To calculate the mean interevent time between two successive events, we consider a system with initial number concentration C_0 and total number N_0 droplets in the simulation. Then, as outlined by Smith and Matsoukas (20), the effective real volume being simulated is N_0/C_0, so that one coagulation event in our (model) system represents C_0/N_0 actual droplets per unit volume. To connect our simulations to real time, we calculate the interevent time by noting that the time between two events is inversely proportional to the sum of the rates of all possible events. If for example k successful events are realized, then the remaining number of droplets in the system is $N_k = N - k$, and the total number concentration of the system C_k is given by

$$\frac{C_k}{C_0} = \frac{N_k}{N_0}.$$

We can then determine the mean interevent time after k coagulations as (20)

$$\Delta T_k = \frac{2N_0}{C_0 \sum_{i=1}^{N_{k-1}} \sum_{j=1}^{N_{k-1}} K_{ij}^F}. \quad [7]$$

In particular, after one droplet coagulation event, we compute the interevent time by

$$\Delta T_1 = \frac{2N_0}{C_0 \sum_{i=1}^{N_0-1} \sum_{j=1}^{N_0-1} K_{ij}^F}, \quad [8]$$

where N_0 is the number of particles represented in the simulation. Introducing the notation $\langle K_{ij}^F \rangle$ for the mean coagulation probability

$$\left\langle K_{ij}^F \right\rangle = \frac{\sum_{i=1}^{N} \sum_{j=1}^{N} K_{ij}^F}{N(N-1)},$$

we can write [7] as

$$\Delta T_k = \frac{2N_0}{C_0 \left\langle K_{ij}^F \right\rangle N_{k-1}(N_{k-1}-1)}.$$

For each droplet we use the interevent time to determine the number of successful enclosure interactions (coagulation-driven growth) before the next droplet coagulation. This unfortunately restricts the time step because modeling the internal state of the droplets requires complete knowledge of enclosure distribution within each droplet.

In an analogous manner to that of the droplets, we also define the mean interevent time for the enclosures in a droplet of volume V as

$$\Delta t = \frac{2V}{\sum_{i=1}^{n-1} \sum_{j=1}^{n-1} K_{ij}^D},$$

where n is the number of the enclosures and n/V is their number density. From this we can now determine how many successful enclosure interactions occur during one droplet coagulation interevent time, ΔT_1, equal to

$$R_1 = \frac{\Delta T_1}{\Delta t}. \quad [9]$$

This number gives an upper bound for the number of successful enclosure interactions because the interevent time for the enclosure interaction increases as the number of the enclosures decreases inside the droplet. Thus, the number of successful enclosure interactions inside the droplet during the time interval ΔT_1 is given by the integer k, which satisfies

$$\sum_{i=1}^{k} \frac{2V}{\left\langle K_{ij}^D \right\rangle (n-i)(n-i-1)} \le \Delta T_1 \le \sum_{i=1}^{k+1} \frac{2V}{\left\langle K_{ij}^D \right\rangle (n-i)(n-i-1)}. \quad [10]$$

On the left-hand side of [10] we have the total time needed for the coagulation of k enclosures and on the right-hand side the total time needed for the coagulation of $k+1$ enclosures. In the next section we describe the accurate computational implementation of the enclosure interaction.

When the number of droplets drops to half the initial value, we replicate the droplets and their internal state. To preserve the physical connection to real time, the topping up process must preserve the average behavior of the system corresponding to the time prior to topping up. In particular, one has to ensure that the characteristic time for droplet collisions stays the same, and doing this requires an increase in the system volume in proportion to the increase in droplets. On the other hand, if the number of enclosures in a droplet becomes too large for the simulation, one can truncate the enclosure system within a droplet by randomly picking a certain number of enclosures and adjusting the corresponding computational volume.

4. IMPLEMENTATION OF HYBRID MC

To implement the numerical computation, we define the coagulation probability by

$$p_{ij} = \frac{K_{ij}^F}{K_{\max}^F},$$

where $K_{\max}^F$ is the maximum value of the coagulation kernel among all droplets. This probability should in principle be normalized by the sum of K_{ij}^F, but the choice of $K_{\max}^F$ is often employed to increase the rate of acceptance. It also has the advantage of saving CPU time because the computation of the sum of k_{ij} over all the enclosures is quite expensive.

A coagulation event is determined to occur only if a randomly drawn number from a uniform distribution is smaller than the probability of the coagulation p_{ij}. If the coagulation is rejected, two new particles are picked and the above steps are repeated until the coagulation condition is satisfied. On successful completion of this step, the selected droplets with volume V_i and V_j are combined to form a new particle with volume $V_i + V_j$ and the total number of the droplets in the computation is decreased by 1. The time increment ΔT is calculated as discussed in the previous section.

Based on the coagulation time of two droplets ΔT_1, the enclosure interactions in each droplet are performed in the following way. After each lth successful enclosure collision in a droplet of volume V, we compute the interevent time for a collision,

$$\Delta t_l = \frac{2V}{\sum_{i=1}^{n-l} \sum_{j=1}^{n-l} \left\langle K_{ij}^D \right\rangle}.$$

If this interevent time is less than ΔT_1, one performs additional collisions until the sum of the interevent enclosure collision times is larger than ΔT_1. As soon as the sum of interevent enclosure collision times becomes larger than ΔT_1, one stops the enclosure coagulation and computes the extra time spent during

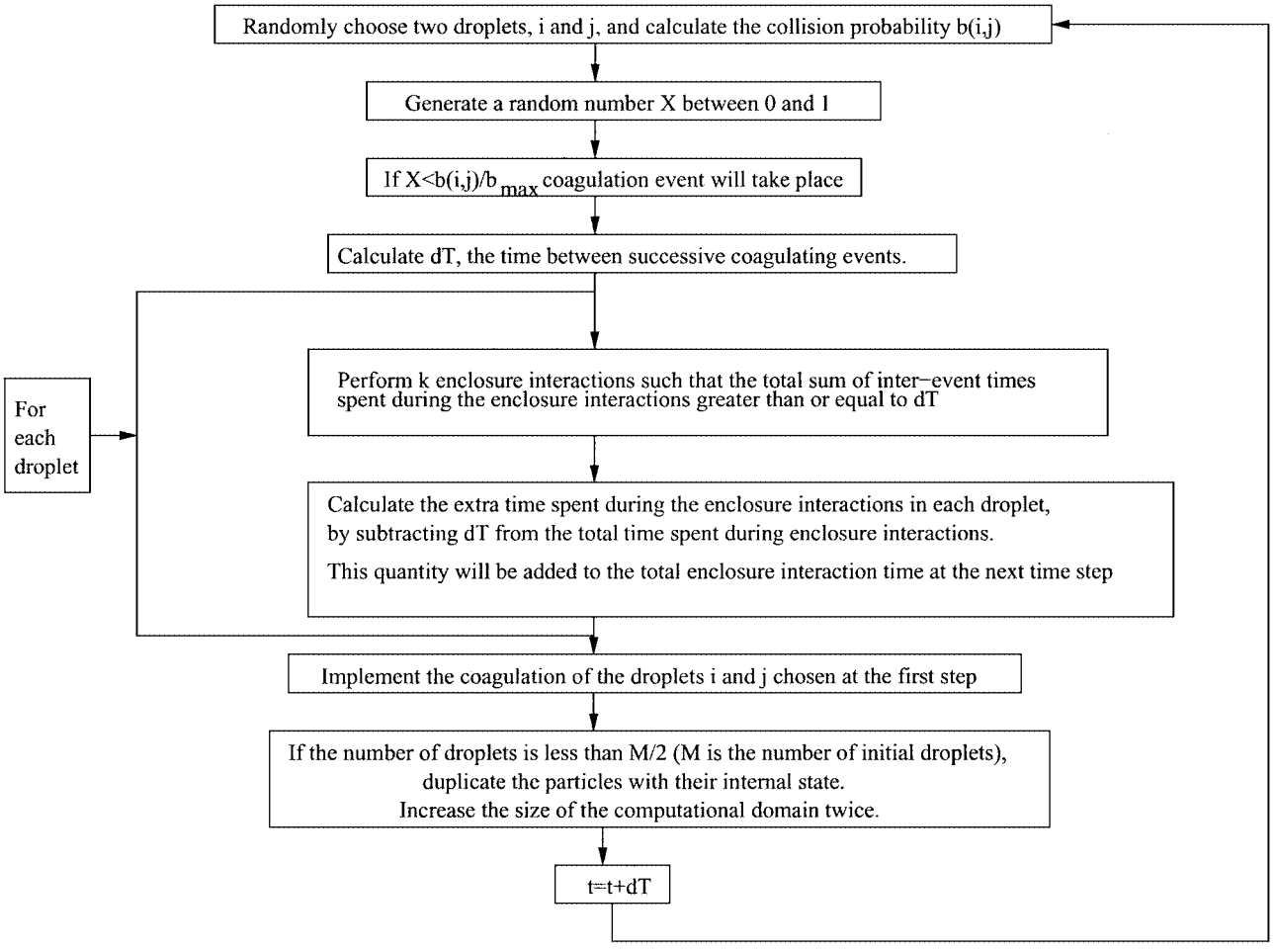

FIG. 3. Flow chart of the hybrid Monte Carlo algorithm.

the enclosure interactions. Assume there were k enclosure interactions with the interevent times Δt_l ($l = 1, 2, \ldots, k$). Then, the extra time spent during the enclosure interactions is defined for each droplet and given by

$$\sum_{l=1}^{k} \Delta t_l - \Delta T_1.$$

This extra time is taken into account at the next time step ΔT_1. In particular, the enclosure coagulation time at the next time step inside the droplet is increased by the amount of extra time. At the end of each time step the extra time spent during enclosure interaction is updated. Moreover, if two droplets collide, then the extra time spent in the resulting droplet is taken to be the sum of the extra times spent in each droplet.

Note that the enclosure interaction in a droplet is performed in the same way as for droplets. The probability of the collision of randomly selected two enclosures i and j is given by

$$p_{ij} = \frac{K_{ij}^D}{K_{\max}^D},$$

where $K_{\max}^D$ is the maximum value of the coagulation kernel among all droplets.

When the number of the droplets are halved, we replicate the droplets and their internal state. A flow chart of our Monte Carlo algorithm is depicted in Fig. 3.

5. SIMULATION RESULTS

We apply the hybrid MC approach to the growth of SiO_2/Fe_2O_3 binary aerosol. We consider a case where we begin with monodisperse droplets of radius $R_0 = 5$ nm and number concentration 10^{12} cm^{-3}. The initial monodisperse enclosure concentration is assumed to be uniform across all droplets.

We consider growth at two temperatures, 2300 and 2600 K, both of which were operating conditions for our experiments. Since silica is the major phase, it is the working fluid whose viscosity will govern the rate of Brownian transport of the minor phase and therefore the growth rate of enclosures. The viscosity of the major component silica (SiO_2) as a function of temperature is given by (21)

$$\mu = 10^{-8.6625\,(1-\frac{3556.03\,\mathrm{K}}{T})}\ \mathrm{kg/ms},$$

and the density of SiO_2 is held constant at $\rho = 5.5$ g/cm^3. From here, we find at $T = 2300$ K

$$K^D = \frac{2kT}{3\mu} = 4.0 \times 10^{-19} \text{ cm}^3/\text{s},$$
$$K^F = \left(\frac{3}{4\pi}\right)^{1/2} \left(\frac{6kT}{\rho}\right)^{1/2} V_0^{1/6} = 6.3 \times 10^{-10} \text{ cm}^3/\text{s}, \quad [11]$$

and at $T = 2600$ K

$$K^D = \frac{2kT}{3\mu} = 1.6 \times 10^{-17} \text{ cm}^3/\text{s},$$
$$K^F = \left(\frac{3}{4\pi}\right)^{1/2} \left(\frac{6kT}{\rho}\right)^{1/2} V_0^{1/6} = 6.7 \times 10^{-10} \text{ cm}^3/\text{s}, \quad [12]$$

where V_0 is the initial volume of the droplets. The reader should note that K^D is a very strong function of temperature, while K^F is essentially temperature independent. The volume fraction $N^\infty V_0$ of droplets is $5e-7$ and the concentration of enclosures in a droplet is taken to $c = 0.2$.

Other variables to specify are the initial number of monodisperse droplets in the simulations and the initial number of monodisperse enclosures in each droplet. We denote this pair by (M, m).

To simulate approximately 100 ms of growth time, it was necessary to top up our system 10 times to maintain reasonable statistics. Numerical computations were run for various sets of (M, m), where M refers to the initial number of the droplets and m refers to the initial number of enclosures in each droplet.

The total number of enclosures in our numerical simulation is equal to $M * m$, which is approximately 3×10^6. To handle such large systems, the code stores and deals with the droplets and their internal state in arrays. In particular, we store all the enclosures in an array, u_i, $i = 1, \ldots, N$, where u_i is the volumes of the enclosures. Then, we define the array for the number of the enclosures in each droplet, n_i, $i = 1, \ldots, n$ and the array for the volume of each droplet V_i, $i = 1, \ldots, n$, where V_i is the volume of the droplets. Here, n is the number of the droplets and N is the total number of enclosures. From this information one can find out which enclosures are contained in a particular droplet. For example, enclosures in jth droplet have indices from $\sum_{l=1}^{j-1} n_l$ to $\sum_{l=1}^{j} n_l$. After each coagulation process we sort the enclosures, u_i, and the droplets, V_i, and calculate new values of n_i. With this structure the code allows us to run simulations with up to 15 million enclosures, on a PC with 256MB RAM and a Pentium III 900-MHz processor, in a few hours. We would like to note that for such a large number of particles the CPU time of sectional models is more favorable, but one needs to remember the limitations of sectional models for binary aerosol coagulation.

Before discussing the simulation results, we would like to make a comment about the use of mean-field equations (in our coagulation constants) for enclosures. One can argue that the description of the enclosures on statistical terms makes sense only if the number of enclosures is sufficiently large. This criticism can be resolved, however, since our system contains a large number of similar droplets. While the behavior of enclosures in a single droplet may not be well described statistically, the behavior of the enclosures in a large number of similar droplets can be described statistically. In that sense we consider the most likely behavior of enclosures in a droplet. We will show later that the behavior of enclosures in each droplet is similar and the mean number of enclosures per droplet increases. Moreover, we would like to note that it would be easy to incorporate a particular dynamics associated with a small number of particles in MC simulations.

In Fig. 4 we plot the mean number of enclosures per droplet (for $T = 2300$ K), i.e., n_{tot}/M_{tot}, where n_{tot} is the total number of enclosures and M_{tot} is the total number of droplets. Results are presented for two sets of initial conditions (M, m), where M refers to the initial number of droplets and m refers to the initial number of enclosures per droplet. The most obvious result of the simulation is that the number of enclosures per droplet relaxes very rapidly from the initial conditions and is followed by a slow increase. This behavior is similar to that observed in our previous works (10, 11). In Appendix A we present a simple model showing that the mean number of enclosures per droplet increases at rate $t^{1/5}$, assuming that the enclosure size distribution is either monodisperse or self-preserving at all times. The slow increase of the mean number of enclosures per droplet can also be understood from the following simple scaling argument. Balancing the characteristic times for enclosure and droplet

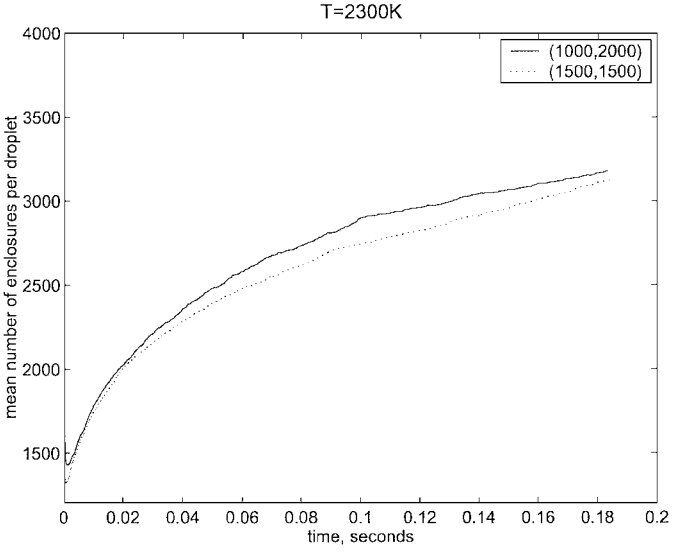

FIG. 4. Mean number of the enclosures per droplet (total number of enclosures/total number of droplets) at $T = 2300$ K for two values of (M, m), where M refers to the initial number of droplets and m refers to the initial number of enclosures per droplet in our simulation. All droplets and enclosures are initially monodisperse.

coagulations, we obtain

$$\frac{1}{K^F N} \sim \frac{\bar{V}}{K^D \bar{n}},$$

where $\bar{V}$ is the mean droplet volume and $\bar{n}$ is the mean number of enclosures per droplet. This balance relationship implies that $\bar{n} \sim K^F \phi / K^D$, where $\phi = N(0)V(0)$ is the volume fraction of the droplets. Since K^F grows as $\bar{V}^{1/6}$, while K^D is independent of the mean volume growth, the above expression for $\bar{n}$ implies that the mean number of enclosures would grow as $\bar{V}^{1/6}$. Further, assuming that the droplet size distribution is self-preserving (or monodisperse), then $\bar{V}^{1/6}$ would grow as $t^{1/5}$ (22).

If we denote $\bar{u}$ as the mean volume of the enclosures and $\bar{V}$ the mean volume of the droplets, then the ratio

$$\frac{n_{tot}\bar{u}}{M_{tot}\bar{V}} = c$$

is constant in our system at all times. This constant for our experimental system was approximately $c = 0.2$. Consequently,

$$\frac{n_{tot}}{M_{tot}} = const \frac{\bar{V}}{\bar{u}}.$$

In the absence of the droplets, the enclosures (would now be the aerosol) coagulate in a free-molecular regime, and their growth rate is proportional to the growth rate of droplets (note that the densities of SiO_2 and Fe_2O_3 are close to each other). More precisely, the growth rate of the enclosures (would now be the aerosol) is $1/c$ times the growth rate of the droplets ($1/c$ represents the ratio of the volume fractions). Thus, $\frac{n_{tot}}{M_{tot}}$ is the relative growth rate of the enclosures due to the presence of the major phase. We see from Fig. 4 that by introducing the major phase, SiO_2, we have effectively moderated the growth rate of the minor phase by some 2000 times (after 30 ms)! We also see from this figure that the asymptotic behavior of the mean number of enclosures per droplet is independent of the initial conditions of (M, m). This latter point implies that, in the asymptotic limit, the aerosol and enclosure growth rate are balanced.

In Fig. 5 we plot the mean number of enclosures per droplet at the higher temperature 2600 K case. Here, because of the lower viscosity of the major phase (silica droplet), the moderation rate is significantly diminished; thus, the coagulation of the enclosures is faster, the average number of enclosures is significantly lower (<100), and therefore the enclosure average volume will be larger. Just as before for the lower temperature conditions, the MC calculations predict the mean number of enclosures per droplet is independent of the initial conditions of the numerical simulation. More important perhaps is that the presence of the major phase can be used as a very significant moderator to nanoparticle growth with the temperature being the control variable (through the viscosity of the major phase).

In Fig. 6 we compare the mean number of enclosures per droplet computed using our MC approach with that calculated in Appendix A. The approach used in the appendix assumes the enclosures are monodisperse at all times. Note that because of variations in enclosure sizes in droplets, the mean number of enclosures per droplet will decrease faster. These results indicate that even though a simple monodisperse model does not allow us to analyze the polydisperse nature of our system, it correctly captures the essence of the long time behavior of the average properties. In Fig. 7 we plot the mean number of the enclosures per droplet on a log–log scale. Clearly, the slope of the increase is $1/5$ on the log–log scale. Finally, we would like to note that the mean number of enclosures per droplet will grow also at the rate

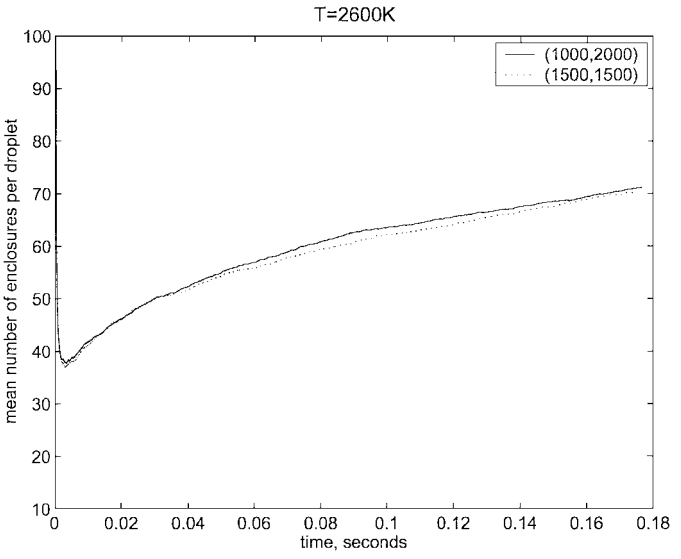

FIG. 5. Mean number of enclosures per droplet (total number of enclosures/total number of droplets) at $T = 2600$ K for two values of (M, m).

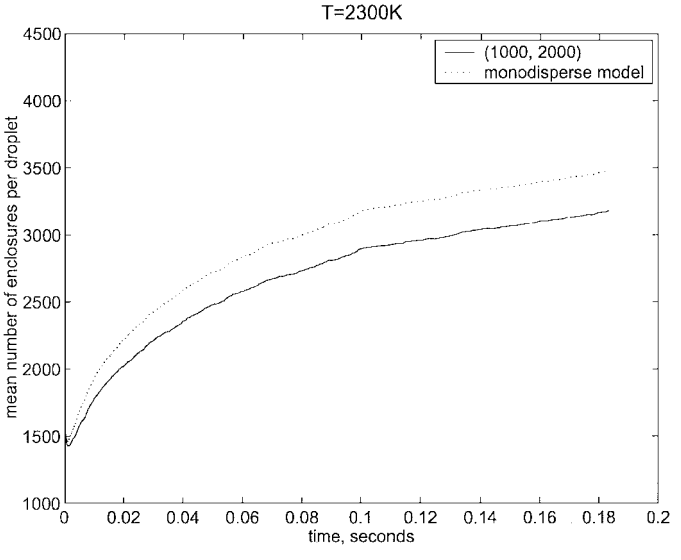

FIG. 6. Mean number of enclosures per droplet (total number of enclosures/total number of droplets) at $T = 2300$ K compared with our simplified model.

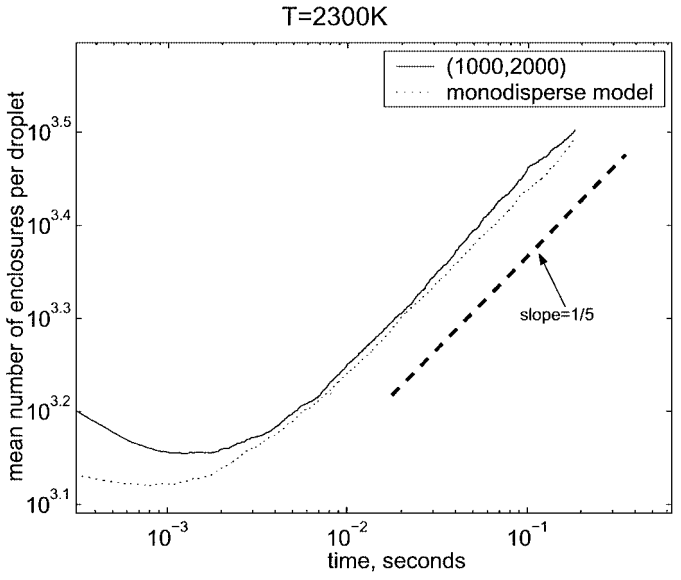

FIG. 7. Mean number of enclosures per droplet (total number of enclosures/total number of droplets) at $T = 2300$ K compared with our simplified model on a log–log scale.

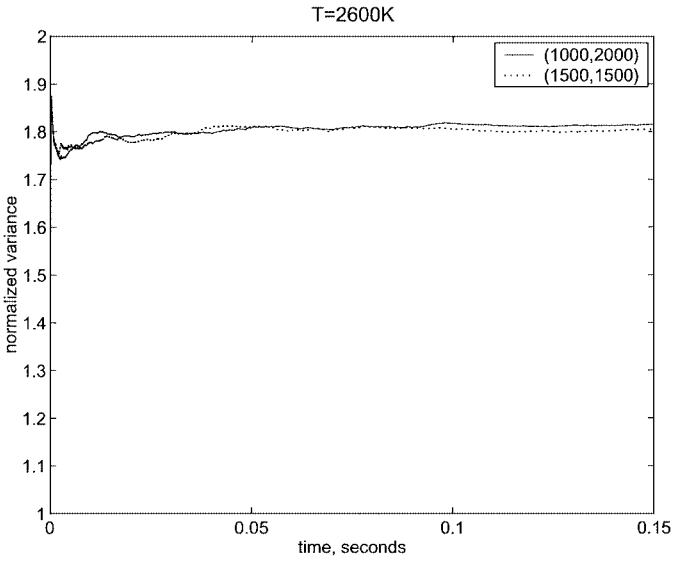

FIG. 9. Normalized second moment $(\overline{u^2}/\bar{u}^2)$ of the enclosures at $T = 2600$ K for two values of (M, m).

1/5 (on a log–log scale) if we assume that both the distribution of droplets and enclosures in a droplet are self-preserving (see Appendix A).

We next consider the characteristics of the enclosure size distribution. In Figs. 8 and 9, we plot the normalized variance, $\overline{u^2}/\bar{u}^2$, of all the enclosures versus time. Here, $\overline{u^2}$ denotes the second moment of the enclosure distribution, defined as

$$\overline{u^2} = \frac{1}{\sum_i n_i} \sum_i n_i u_i^2,$$

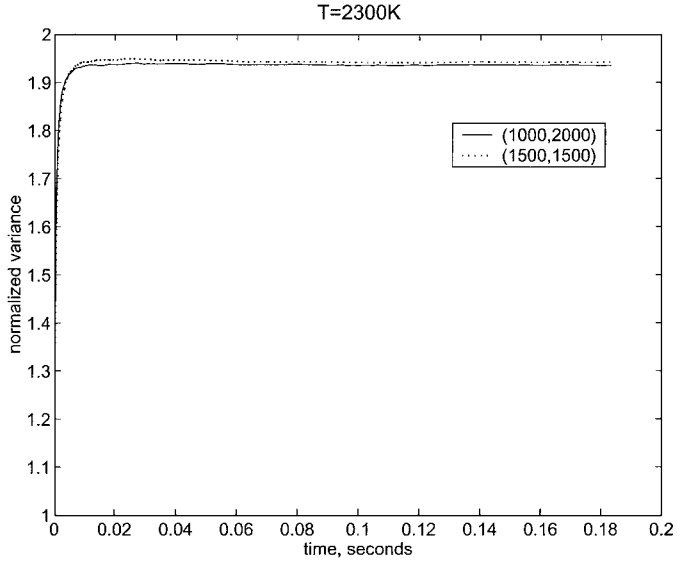

FIG. 8. Normalized second moment $(\overline{u^2}/\bar{u}^2)$ of the enclosures at $T = 2300$ K for two values of (M, m).

and $\bar{u}$ denotes the first moment of the enclosure distribution, defined as

$$\bar{u} = \frac{1}{\sum_i n_i} \sum_i n_i u_i,$$

where n_i is the number of the enclosures with volume u_i. In all simulations the normalized variance approaches an asymptotic value, implying that the enclosures reach a so-called "self-preserving" size distribution. In a lower temperatures setting, $T = 2300$ K, the normalized variance approaches the asymptotic value much faster than at $T = 2600$ K. This is associated with the fact that the mean number of enclosures per droplet is much higher at 2300 K. In the end of this section we will discuss this issue. The higher temperature 2600 K case (Fig. 9) also shows some noise at initial times and is associated with the numerical error in the MC simulation, which is proportional to $1/\sqrt{n}$, where n is the number of enclosures. The higher temperature case involves a much lower number of enclosures per droplet (as low as 50) and a correspondingly small total number of enclosures and therefore more error in the computation.

We next turn our attention to the average volume of enclosures, plotted in Fig. 10 as a function of time at 2300 K. This quantity is normalized by the initial enclosure volume, 0.05 nm^3. Note that the initial enclosure size depends on the number of particles in a droplet at $t = 0$. The MC results show that volume growth is independent of the initial conditions and are linear functions of time and with the same dependence expected for an aerosol undergoing coagulation in a continuum regime (23); see also Appendix B, [19]. In Fig. 11 we compare the growth of the average volume of the enclosures at the two different temperatures. The results clearly indicate that the growth of

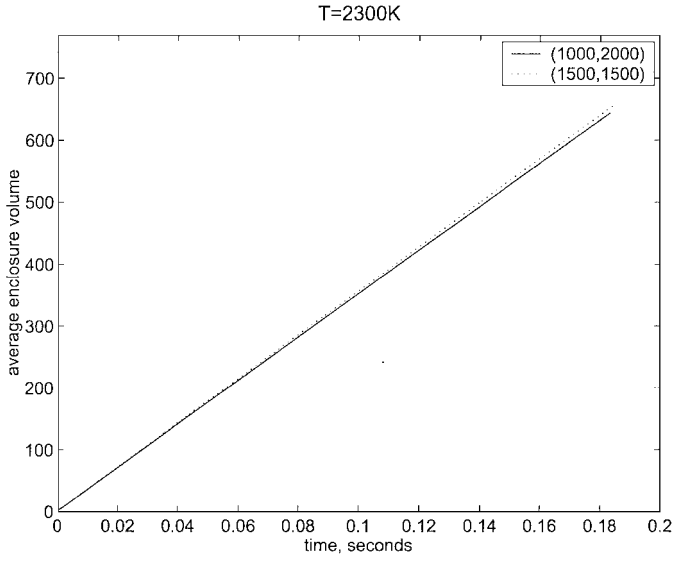

FIG. 10. Average normalized volume of enclosures at $T = 2300$ K for two values of (M, m).

enclosures is much slower for the lower temperature case because of the higher droplet viscosity. Indeed, this is the crucial result in the whole concept of using a matrix to moderate the growth of nanoparticles. In this example, only a 300 K change in temperature results in a several orders of magnitude change in enclosure volume! Such a change in growth rate could never have been achieved for a purely coagulating aerosol.

In Figs. 12 and 13, we present the enclosure size distribution at different times by plotting the dimensionless enclosure size distribution $\psi(\eta) = \frac{n(u,t)\bar{u}}{n^{\infty}}$ versus the dimensionless volume $\eta = u/\bar{u}$, where n^{∞} is the total number of enclosures. Clearly, the distributions have already collapsed onto a self-preserving

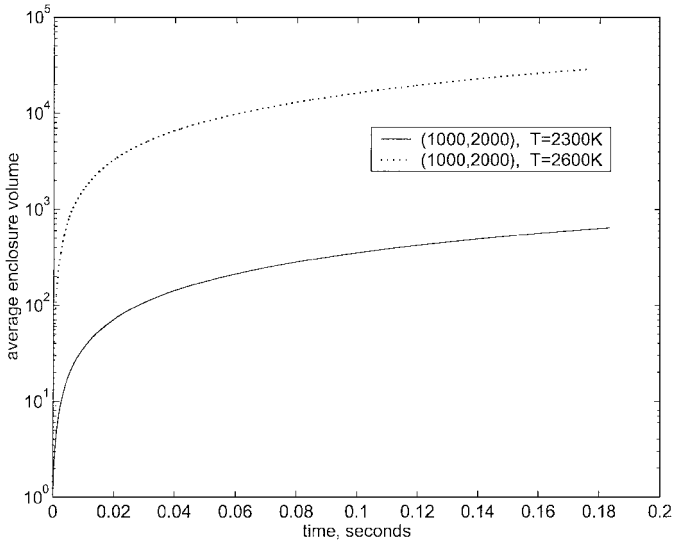

FIG. 11. Comparison of the average volume of the enclosures at $T = 2300$ K and $T = 2600$ K. Note a log scale along the vertical axis.

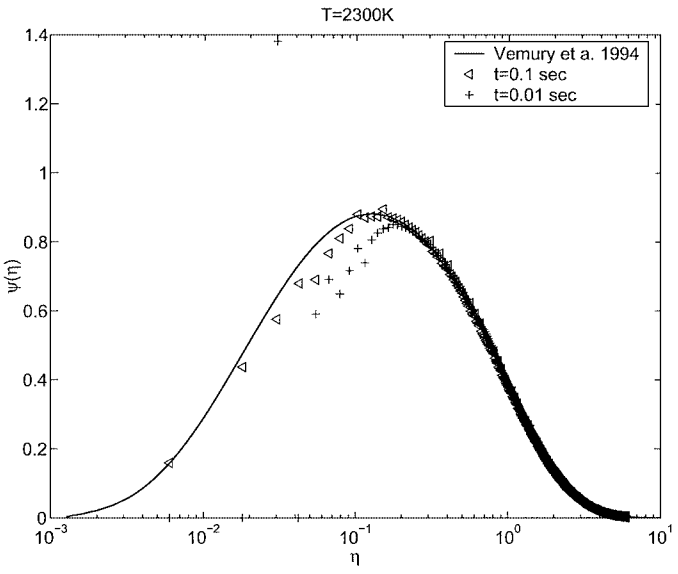

FIG. 12. The enclosure size distribution at $T = 2300$ K. Dimensionless number density, $\psi(\eta) = \frac{n(u,t)\bar{u}}{n^{\infty}}$ versus dimensionless volume, $\eta = u/\bar{u}$. The numerical values of the self-preserving distribution for the Brownian regime (solid line) is taken from Vemury *et al*. (24).

form for coagulation in a continuum regime (the numerical values of $\psi(\eta)$ are taken from Vemury *et al*. (24)) at $T = 2300$ K. While at 2600 K the enclosure size distribution is clearly narrower. This is associated with a small number of enclosures per droplet and will be explained at the end of this section. In Fig. 15 we plot the enclosure size distribution at very large times to show that the enclosure size distribution approaches

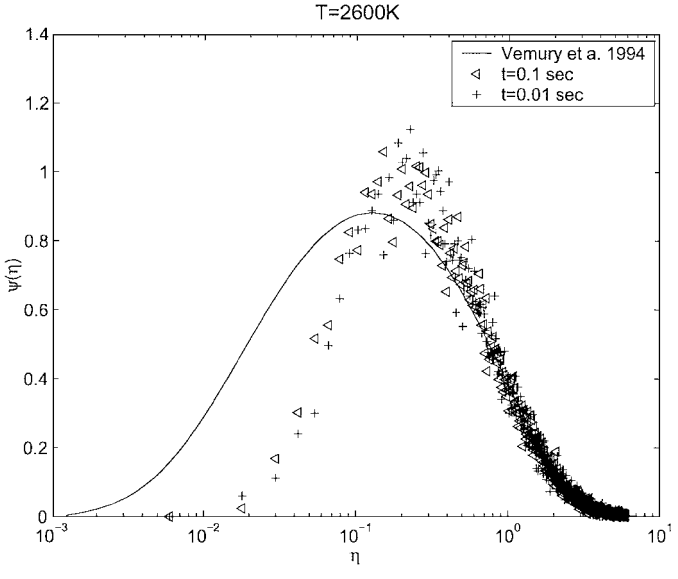

FIG. 13. The enclosure size distribution at $T = 2600$ K. Dimensionless number density, $\psi(\eta) = \frac{n(u,t)\bar{u}}{n^{\infty}}$ versus dimensionless volume, $\eta = u/\bar{u}$. The numerical values of the self-preserving distribution for the Brownian regime (solid line) is taken from Vemury *et al*. (24).

the self-preserving form for Brownian coagulation. The convergence of the enclosure size distribution to the self-preserving form for Brownian coagulation depends on the mean number of enclosures per droplet and will also be discussed in more detail at the end of this section.

It is clear that if the number of the enclosures per droplet becomes too small, one (or two) enclosure(s) per droplet, for example, (this will happen if the temperature is very high, e.g., $T = 3200$ K), then the enclosure size distribution will be very similar to the droplet size distribution (free molecule) provided that the total volume of the enclosures in a droplet is the same for all the droplets. Under such conditions, since the enclosures grow at the rate of the aerosol, the use of a matrix (major phase) has no value. This places a requirement on the use of a matrix that has sufficient viscosity to moderate the enclosure growth rate.

The numerical results show that the enclosure distribution collapses onto the self-preserving size distribution, which is close to the Brownian self-preserving size distribution if the mean number of the enclosures per droplet is large. In Appendix B we show that if the mean enclosure volumes of each droplet are approximately the same, then the enclosure size distribution is self-preserving in each droplet, and the form of the self-preserving function is the same for all the droplets. Thus, this self-preserving function has to be the self-preserving function corresponding to the coagulation kernel of the continuum regime. In general, the mean enclosure volumes of each droplet are not the same.

Next, we study the statistics of the mean enclosure volumes of each droplet. The behavior of this quantity would offer some keys to the convergence to the self-preserving size distribution of enclosures at different temperatures. We define the mean enclosure volume of each droplet in the following way. For each droplet i with volume V_i, total enclosure volume, U_i, and number of enclosures, n_i, the mean enclosure volumes of each droplet is defined as $\bar{u}_i = U_i/n_i$. Note that in, our numerical simulations, $U_i = cV_i$, where c is the same for all droplets. Then, $\bar{u}_i = cV_i/n_i$.

In Fig. 14 we plot the normalized variance of mean enclosure volumes of each droplet, $\bar{u}_1, \ldots, \overline{u_M}$, where M is the number of droplets (in this case (1000, 2000) is chosen). The normalized variance is then defined as $\overline{u_m^2}/\overline{u_m^2}$, where

$$\overline{u_m^2} = \frac{1}{\sum_i m_i} \sum_i m_i \bar{u}_i^2, \quad \overline{u_m} = \frac{1}{\sum_i m_i} \sum_i m_i \bar{u}_i,$$

where m_i is the number of the mean enclosure volumes with volume $\bar{u}_i$. The interesting observation is that the normalized variance of the mean enclosure volumes of each droplet is quite sensitive to the temperature and is much smaller if the mean number of enclosures per droplet is larger, as is the case when the temperature is low (i.e., internal transport is slow). Indeed, at the highest temperatures, 3200 K, there is on average only 1–2 enclosures per droplet at a time scale of 1 s; thus, the mean enclosure

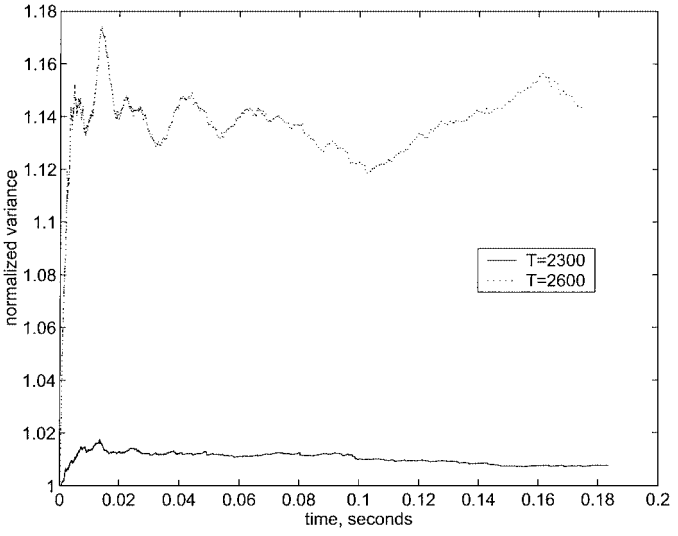

FIG. 14. The normalized variance $(\overline{u_m^2}/\overline{u_m^2})$ of the mean enclosure volumes of each droplet at different temperatures.

volumes of each droplet simply track the droplet volumes, i.e., reach the self-preserving size distribution corresponding to the free-molecule regime. At the lowest temperatures ($T = 2300$ K) the mean enclosure volumes are essentially equivalent between droplets. Under these conditions the coagulation of the droplets does not influence the enclosure size distribution; thus, if the mean number of the enclosures per droplet is large enough, the self-preserving form of the enclosure distribution is approximately the same as that corresponding to coagulation in a continuum regime. Note that at $T = 2600$ K the normalized variance of mean enclosure volumes of each droplet eventually will become very close to unity (see discussion in the next paragraph).

The behavior of the normalized variance of mean enclosure volumes of each droplet can be explained, we believe, in the following way. At an asymptotic condition, the characteristic interaction times for the enclosures in each droplet are balanced with the characteristic coagulation time for the droplets. The characteristic interaction (i.e., coagulation) time for the enclosures in each droplet V_i is given by

$$t_i^c = \frac{V_i}{K^D n_i} \qquad [13]$$

and is constant for all droplets. Since the total enclosure volume of a droplet with volume V_i is cV_i, t_i^c can be written as

$$t_i^c = \frac{\bar{u}_i}{cK^D},$$

where $\bar{u}_i$ is the mean volume of the enclosures of the droplet. So at an asymptotic limit we expect the mean enclosure volumes of each droplet to be constant, i.e., the normalized variance to be equal to unity. However, this characteristic time [13] is only defined if $n_i > 1$. So if the number of enclosures per droplet

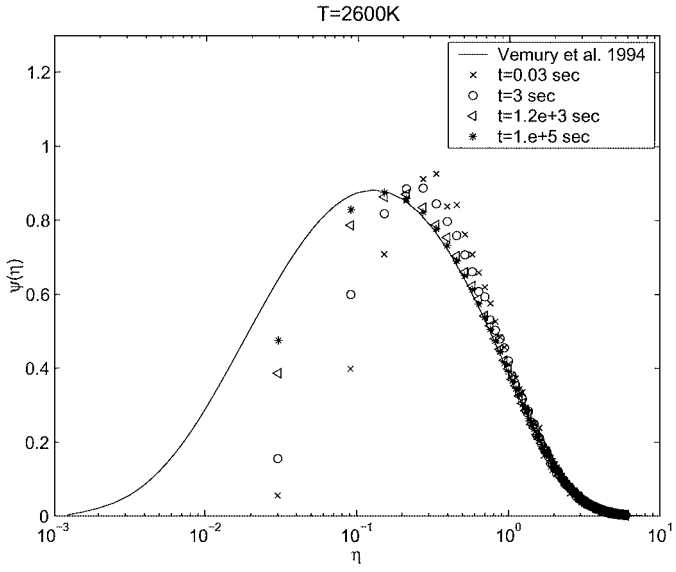

FIG. 15. The enclosure size distribution at large times for $T = 2600$ K. Dimensionless number density, $\psi(\eta) = \frac{n(v,t)\bar{v}}{n^{\infty}}$ versus dimensionless volume, $\eta = v/\bar{v}$. The numerical values of the self-preserving distribution for the Brownian regime (solid line) is taken from Vemury *et al*. (24). The mean number of enclosures per droplet at these time instants are $\bar{n}(0.03\,\mathrm{s}) = 50$, $\bar{n}(3\,\mathrm{s}) = 100$, $\bar{n}(1.2e+3\mathrm{s}) = 1200$, and $\bar{n}(1e+5\,\mathrm{s}) = 2000$.

is close to unity, the characteristic enclosure coagulation times (defined in [13]) in each droplet will in general not be equal to each other and we need to take account of the variation in number of enclosures per droplets. If this variance is large, then there are many droplets with a small number (close to unity) of enclosures when the mean number of enclosures per droplet is also small. This is the case (based on our numerical observations, which will not be presented here) for $T = 2600$ K up to 100 ms. In Fig. 15 we present the enclosure size distribution at large times for $T = 2600$ K. The enclosure size distribution approaches the Brownian self-preserving size distribution, albeit very slowly. Note that the mean number of enclosures per droplet plays an important role in this convergence. As we see from Fig. 15, if the mean number of enclosures becomes larger than a few thousand, then the enclosure size distribution is approximately the same as the self-preserving form of Brownian coagulation. However, the mean number of enclosures per droplet grows slowly (as $t^{1/5}$); thus, it takes a long time for the mean number of enclosures to reach a few thousand at high temperatures.

6. CONCLUSIONS

In this paper we have presented a hybrid Monte Carlo technique to simulate the simultaneous coagulation and kinetically controlled phase segregation of two-component immiscible aerosols. The hybrid MC combines two MC simulations. One simulates the coagulation of droplets and the other simulates the interaction between enclosures, based on a mass-transfer limited growth. The method was applied to the SiO_2/Fe_2O_3, binary system that we have studied in our previous work (10, 11). The hybrid MC approach allows us to compute the average properties of our system, including mean number of enclosures per droplet, average enclosure volume, and the normalized second moment of the enclosures. The results indicate that the asymptotic behavior is independent of the initial conditions of our numerical simulations and indicates that our MC approach is robust.

The mean number of enclosures per droplet is a measure of the relative growth rate of the enclosures due to the presence of the droplets. The computations show that this quantity increases at a slow rate and that the asymptotic behavior is independent of initial conditions with regard to initial droplet and enclosure size. Temperature, on the other hand, is an extremely important variable since it has a very significant impact on the intradroplet transport process while it is relatively insensitive to the droplet coagulation rate. The computations on the statistics of enclosure size distribution indicate that the enclosure size distribution reaches a self-preserving condition at large times, which is very close to the self-preserving distribution for Brownian coagulation, if the mean number of enclosures per droplet is large (i.e., that is, if the temperature is not high or the viscosity of the liquid droplet is not too low). Higher temperatures require longer times for the enclosure distribution to reach the self-preserving condition.

Using our MC approach, we also study the mean enclosure volumes of each droplet and their distribution. We show that the normalized variance of the mean enclosure volumes of each droplet is very small if the mean number of enclosures per droplet is high. This shows that the size distribution of mean enclosure volumes of each droplet is not correlated to the size distribution of the droplets at low temperatures (or when the mean number of the enclosures per droplet is high). We note that the latter statistics are only possible with a model that does not assume any a priori enclosure distribution.

One of the main advantages of our MC approach over the sectional models is that the MC framework introduced here is amenable to the inclusion of additional phenomena including the addition of new mass to the system through nucleation as well as the imposition of thermodynamic constraints, in addition to the kinetic ones discussed above for both droplet and enclosure growth.

Finally, the results indicate that the use of a major/minor phase combination may be a useful strategy in controlling the growth rate of nanoparticles in the minor phase by controlling the nanoparticle encounter frequency. We noted for example that the encounter frequency for our silica/iron oxide system the iron oxide growth could be moderated (decreased) under experimental conditions.

APPENDIX A: MONODISPERSE MODEL

Assume that the enclosure coagulation in a droplet of volume V satisfies

$$\frac{d(n/V)}{dt} = -2K^D(n/V)^2, \qquad [14]$$

where n is the number of enclosures in the droplet. Equation [14] holds if the enclosures are monodisperse or have self-preserving size distribution. In the latter case K^D should be replaced by $1.075\,K^D$ (22). Integrating [14],

$$\frac{1}{n(t)} = \frac{1}{n(0)} + 2\frac{K^D}{V}t. \qquad [15]$$

Further assume that the total volume of the enclosures in each droplet is cV, where c is the same for all the droplets. Then, multiplying [15] by cV, we obtain

$$\bar{u}(t) = \bar{u}(0) + 2cK^D t, \qquad [16]$$

where $\bar{u}(t)$ is the mean enclosure volume in a droplet at time instant t. [16] indicates that the growth of mean volume of the enclosures is independent of droplet volume. Further, we note that a collision of two droplets with the equal mean enclosure volume results in a droplet whose mean enclosure volume is the same as those prior to the collision. Thus, if we assume that initially all enclosures are monodisperse with the same volume, then the mean volume of the enclosures (assuming them to be monodisperse at later times) will remain the same for all droplets. From here the number of enclosures in a droplet of volume V is given by

$$n_V(t) = \frac{cV}{\bar{u}(t)}.$$

Then, the mean number of the enclosures per droplet is defined as

$$\bar{n} = \frac{c\bar{V}}{\bar{u}(t)}. \qquad [17]$$

[17] is also true if the enclosure distribution in the droplet is self-preserving. Indeed, using Appendix B, we can show that if the enclosure size distribution is self-preserving and if the mean volume of the enclosures of each droplet is the same, then the enclosure size distributions remain self-preserving; i.e., the total number of enclosures in a droplet of volume V satisfies [14]. Then, the mean enclosure volume in each droplet will be equal at later times according to [15]. This fact demonstrates the validity of the simple model when the size distribution of enclosures is self-preserving.

To find an expression for $\bar{V}$ (mean droplet volume growth), we can assume that the droplets have self-preserving size distribution. Then, following (22, Sect. 7),

$$\frac{dN(t)}{dt} = -\frac{\alpha}{2}\left(\frac{3}{4\pi}\right)^{1/6}\left(\frac{6kT}{\rho}\right)^{1/2}\phi^{1/6}N^{11/6}(t), \qquad [18]$$

where $\alpha \approx 6.67$ and $\phi = N(0)V(0)$ is the volume fraction. From [18] one can easily find the expression for the volume growth, and consequently the expression for the mean number of enclosures per droplet

$$\bar{n} = c\frac{\left(V^{5/6}(0) + 6/5K_0^F\phi t\right)^{6/5}}{\bar{u}(0) + 2cK^D t},$$

where $K_0^F = \frac{\alpha}{2}(\frac{3}{4\pi})^{1/6}(\frac{6kT}{\rho})^{1/2}\,\phi^{1/6}$. Note that as $t \to \infty$, $\bar{n}(t) \sim t^{1/5}$.

APPENDIX B: SELF-PRESERVING DISTRIBUTION OF THE ENCLOSURES

In this appendix we show that if the distribution of the enclosures is self-preserving in each droplet and if the mean volume of the enclosures in each droplet is the same at some time t_0, then the enclosure distribution in each droplet will remain self-preserving and their mean volume will be the same for all the droplets at all times $t > t_0$. This follows from the following three statements:

(1) *As a result of the coagulation of two droplets, the mean volume of the enclosures in the resulting droplet does not change if before the collision the mean volume of the enclosures in each droplet was the same.*

(2) *The enclosure coagulation in each droplet changes the mean volume in the same way for all the droplets if the enclosure distribution in the droplets is self-preserving.*

If the distribution is self preserving, we have (22)

$$n(v,t) = \psi(\eta)\frac{n^\infty}{\bar{v}},$$

where $\eta = v/\bar{v}$. The function $\psi(\eta)$ is the same for all the droplets. The total number of enclosures in each droplet is defined by

$$\frac{dn^\infty}{dt} = -\frac{2kT}{3\mu V}(1+ab)(n^\infty)^2,$$

where $a = \int_0^\infty \eta^{1/3}\psi(\eta)$ and $b = \int_0^\infty \eta^{-1/3}\psi(\eta)$ and V is the volume of the droplet. Or

$$\frac{dn^\infty}{dt} = -\frac{\sigma^B}{V}(n^\infty)^2,$$

where $\sigma^B = \frac{2kT}{3\mu}(1+ab)$ is the same constant for all the droplets. Solving this equation,

$$\frac{1}{n^\infty(t)} = \frac{1}{n^\infty(0)} + \frac{\sigma^B}{V}t.$$

Multiplying this equation by the total volume of the enclosures, which is cV, where c is the same for all the droplets, we have

$$\overline{v(t)} = \overline{v(0)} + c\sigma^B t. \quad [19]$$

Thus, if $\overline{v(0)}$ is the same for all the droplets, then $\overline{v(t)}$ also remains the same.

(3) *The distribution of the enclosures during the collision of the droplets will remain self-preserving.*

Assume two droplets with enclosure distribution $n_1(v, t)$ and $n_2(v, t)$ collide. Since the enclosure distribution in both droplets is self-preserving and the mean volume of the enclosures in the droplets is equal, we have

$$n_1(v, t) = \psi(n)\frac{N_1^\infty(t)}{\bar{v}}, \quad n_2(v, t) = \psi(\eta)\frac{N_2^\infty(t)}{\bar{v}}.$$

The resulting enclosure distribution is

$$n(v, t) = n_1(v, t) + n_2(v, t) = \psi(\eta)\frac{N^\infty(t)}{\bar{v}},$$

where $N^\infty(t) = N_1^\infty(t) + N_2^\infty(t)$. Thus, the resulting distribution is the self-preserving.

ACKNOWLEDGMENTS

The authors thank Dr. H. Struchtrup (University of Victoria) for helpful discussions and comments.

REFERENCES

1. Biswas, P., Yang, G., and Zachariah, M. R., *Combust. Sci. Technol.* **134,** 183 (1998).
2. Biswas, P., and Zachariah, M. R., *Environ. Sci. Technol.* **31,** 2455 (1997).
3. Ehrman, S., Aquino-Class, M., and Zachariah, M. R., *J. Mater. Res.* **14,** 1664 (1999).
4. Ehrman, S., Friedlander, S. K., and Zachariah, M. R., *J. Aerosol Sci.* **29,** 687 (1998).
5. Ehrman, S., Friedlander, S. K., and Zachariah, M. R., *J. Mater. Res.* **14,** 4551 (1999).
6. Zachariah, M. R., Aquino-Class, M., Shull, R., and Steel, E., *Nanostruct. Mater.* **5,** 383 (1995).
7. McMillin, B. K., Biswas, P., and Zachariah, M. R., *J. Mater. Res.* **11,** 1552 (1996).
8. Biswas, P., Wu, C., Zachariah, M. R., and McMillen, B. K., *J. Mater. Res.* **12,** 714 (1997).
9. Zachariah, M. R., Shull, R., McMillin, B. K., and Biswas, P., *Nanotechnology* **622,** 42 (1996).
10. Efendiev, Y., Luskin, M., Struchtrup, H., and Zachariah, M. R., *J. Nanoparticle Res.*, in press.
11. Struchtrup, H., Luskin, M., and Zachariah, M. R., *J. Aerosol Sci.* **32,** 1479 (2001).
12. Gillespie, D., *J. Atmos. Sci.* **32,** (1975).
13. Rosner, D., and Yu, S., *AIChE J.* **47,** 545 (2001).
14. Scott, W., *J. Atmos. Sci.* **24,** 221 (1967).
15. Shah, B., Ramakirishna, D., and Borwanker, J., *AIChE J.* **23,** 897 (1977).
16. Spouge, J., *J. Colloid Interface Sci.* **107,** 38 (1985).
17. Tandon, P., and Rosner, D., *J. Colloid Interface Sci.* **213,** 273 (1999).
18. Norris, J., *Ann. Appl. Prob.* **9,** 78 (1999).
19. Liffman, K., *J. Comput. Phys.* **100,** 495 (1992).
20. Smith, M., and Matsoukas, T., *Chem. Eng. Sci.* **53,** 1777 (1998).
21. Jans, G., Lakshminarayanan, F. D. G., Lorentz, P., and Tomkins, R., "*Molten Salts: Volume 1, Electrical Conductance, Density, and Viscosity Data*," U.S. National Standard Reference Data Series, U.S. National Bureau of Standards, Washington, DC, 1968.
22. Friedlander, S. K., "*Smoke, Dust, and Haze*." Oxford Univ. Press, Oxford, 2000.
23. Friedlander, S. K., and Wang, C., *J. Colloid Interface Sci.* **22,** 126 (1966).
24. Vemury, S., Kusters, K., and Pratsinis, S., *J. Colloid Interface Sci.* **165,** 53 (1994).